Automatic detection of particle size distribution by image analysis based on local adaptive canny edge detection and modified circular Hough transform

Yingchao Meng[a,1], Zhongping Zhang[b,1], Huaqiang Yin[a], Tao Ma[a,*]

[a] Institute of Nuclear and New Energy Technology, Key Laboratory of Advanced Reactor Engineering and Safety of Ministry of Education, Tsinghua University, Beijing 100084, China
[b] Department of Electrical and Computer Engineering, University of Rochester, Rochester, New York 14642, USA

ARTICLE INFO

ABSTRACT

To obtain size distribution of nanoparticles, scanning electron microscope (SEM) and transmission electron microscopy (TEM) have been widely adopted, but manual measurement of statistical size distributions from the SEM or TEM images is time-consuming and labor-intensive. Therefore, automatic detection methods are desirable. This paper proposes an automatic image processing algorithm which is mainly based on local adaptive Canny edge detection and modified circular Hough transform. The proposed algorithm can utilize the local thresholds to detect particles from the images with different degrees of complexity. Compared with the results produced by applying global thresholds, our algorithm performs much better. The robustness and reliability of this method have been verified by comparing its results with manual measurement, and an excellent agreement has been found. The proposed method can accurately recognize the particles with high efficiency.

1. Introduction

Nanoparticles have gained a lot of attention because of their special characteristics, such as small size effect, surface effect, quantum effect and macro-quantum tunnel effect, which enables them unique chemical (Baudouin et al., 2013; Reske et al., 2014) and physical (Houshiar et al., 2014; Mohammadi et al., 2013) properties. They can be applied in various fields including material fabrication (Pandey et al., 2013; Tanhaei et al., 2015), drug delivery (Blanco et al., 2015; Couvreur, 2013), gene detection (Chinen et al., 2015; Shi et al., 2015) and so on. The size distribution of the nanoparticles is a primary concern both for research and for application, and nanoparticles with narrow size distribution are highly desired.

In order to obtain the size distributions of nanoparticles, scanning electron microscope (SEM) and transmission electron microscopy (TEM) have been adopted as an effective tool to characterize the microstructure of the nanoparticles. SEM mainly uses a focused beam of electrons to intact with the surface of specimens to generate various signals to form image, while TEM mainly collects the electrons that transmit through specimens to form images, both of which can produce micrographs approaching nanoscale. To get the statistically meaningful size distribution from the micrographs, hundreds of particles need to be measured. Currently, the particle size is usually measured manually

(Dastanpour and Rogak, 2014; Lovell et al., 2015; Trandafilović et al., 2012), which is extremely time-consuming and labor-intensive. In addition, manual measurement can also be affected by human intervention (Woehrle et al., 2006). Therefore, it is necessary to develop other efficient, accurate and objective approaches to automatically measure the particle size.

Many automatic image processing algorithms have been developed to provide much more accurate measurement of large numbers of particles from the microscopy images. Wu and Yu (2012) has analyzed the particle size with the assistance of image processing algorithms, but they are not suitable for qualifying the sizes and distributions of nanoparticles. Based on watershed segmentation, a semi-automatic image processing method has been proposed by De Temmerman et al. (2014) to recognize the minimal size in one dimension of primary particles in aggregated nanomaterials. Dastanpour et al. (2016) has developed a 2-D pair correlation function to analyze nanoparticle aggregates from TEM images, but only the mean primary particle diameter can be obtained by this method. One of the most recent studies has been conducted by Mirzaei and Rafsanjani (2017). They have developed an image processing algorithm based on several pre-processing techniques and circular Hough transform (CHT) to directly get the size distribution of nanoparticles from the micrographs. CHT is a powerful method to detect circular objects, which has been studied extensively

---
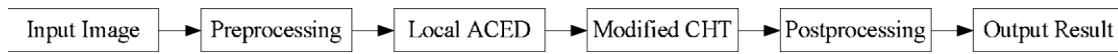
Fig. 1. Block diagram of the proposed algorithm.
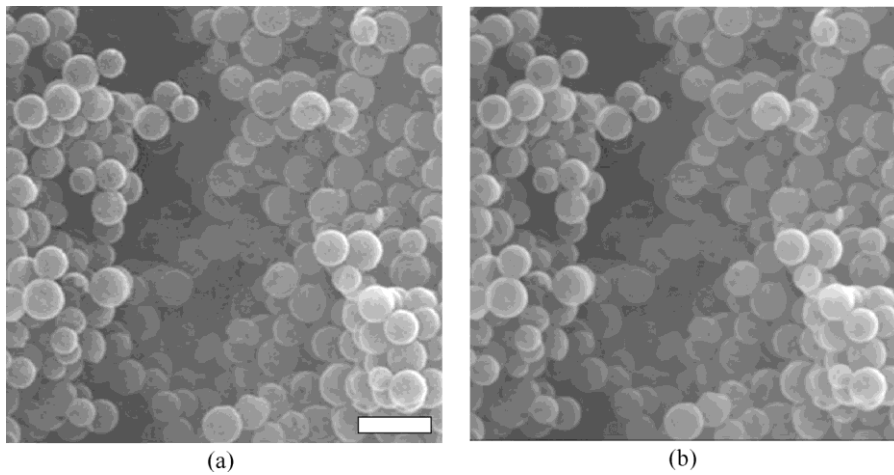
Fig. 2. (a) Original image of porous hollow carbon nanospheres (He et al., 2013). (b) Image after preprocessing. Scale bar = 400 nm.
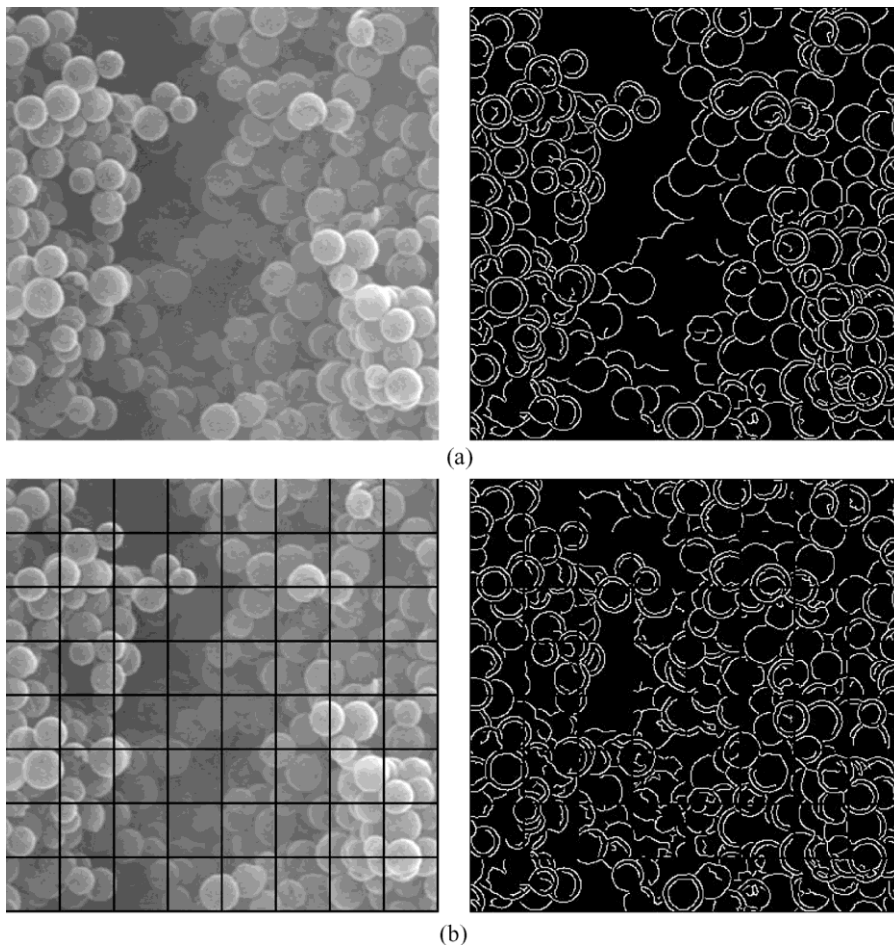
Fig. 3. (Left column) (a) Image without any segmentation. (b) Image segmented into 8×8. (Right column) The corresponding binary edge detection results.

(Lappalainen and Lehmonen, 2012; Pei and Horng, 1995; Rizon et al., 2005; Smereka and Duleba, 2008; Yuen et al., 1990). However, in their studies, the binary results are obtained by adopting a single global threshold value to process the entire image. Indeed, good results can be obtained if the edge pixels of the particles show a sufficiently different intensity from the background. But for most cases, the gray level, noise and illumination for different parts of a same image vary significantly,

which makes it really impractical to get a good binary result by setting a single specific value for thresholding the whole image. To address the problem, local attributes must be taken into consideration. Many groups have conducted researches on image processing based on local attributes (Hemachander et al., 2006; Cervera et al., 2011; Sun and Cai, 2014), the results of which have demonstrated its benefits for dealing with complex images. Hence, to detect particles from images with high
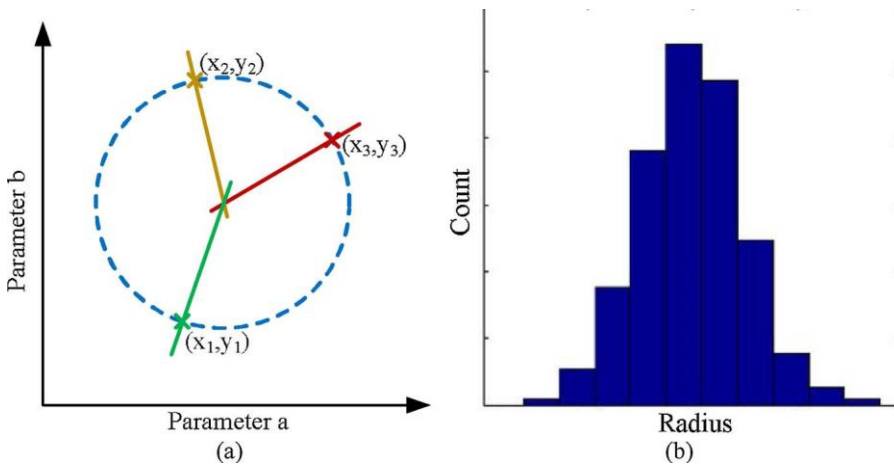
Fig. 4. Two stages of the modified CHT. In (a), a 2D Hough Transform is established by edge detection information to find circle center coordinates. In (b), a radius histogram is plotted to find the most reasonable radius of the circle.
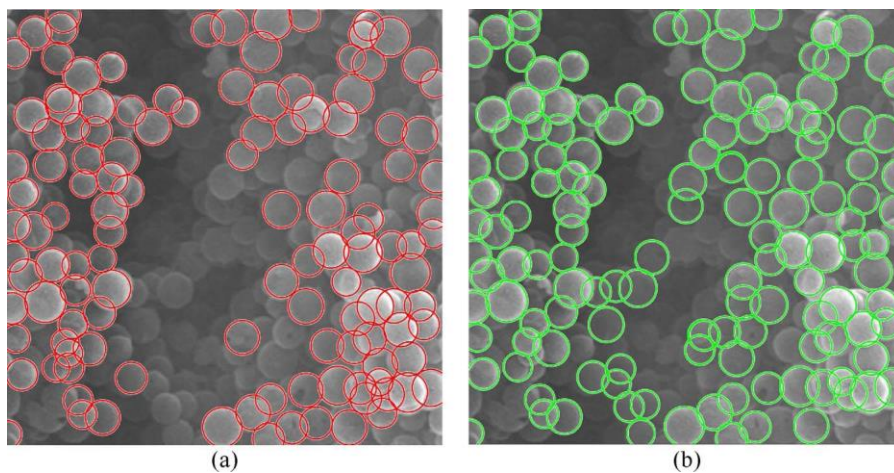
Fig. 5. (a) Overlapped image of the original image and the result by applying modified CHT to Fig. 3a. (b) Overlapped image of the original image and the result by applying modified CHT to Fig. 3b.
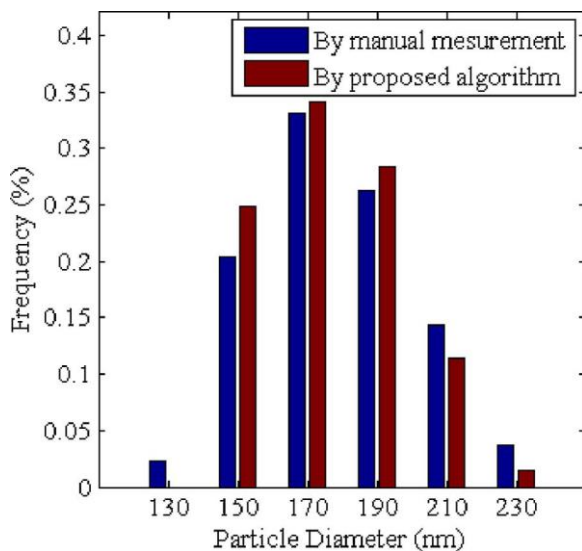
Fig. 6. Comparison of the particle size distributions by manual measurement and by our algorithm.

complexity, an algorithm which can utilize local thresholds is developed.

In this paper, a simple image processing algorithm based on local adaptive Canny edge detection (ACED) and modified CHT is presented. The proposed method can rapidly measure the particle size distribution with high precision. The local ACED can segment the image into many square sub-images and automatically find the local high and low threshold values of each sub-image for further edge detection. Compared with the global ACED which utilizes the global threshold values of the whole image, a much better binary result with more edge characteristics can be obtained. The obtained binary result will be further analyzed by modified CHT to detect circular particles. The reliability and robust of the proposed algorithm are verified by comparing its results with manual measurement data.

2. Proposed methodology

Fig. 1 presents a simplified block diagram of the proposed algorithm. SEM and TEM are very sensitive to instrumental and environmental disturbances, such as mechanical vibration, magnetic field interference, power supply instability and so on, which can introduce many noises to the recorded images (Jones and Nellist, 2013; Muller et al., 2006). Therefore, before applying local ACED, graying and denoising are adopted in image preprocessing step to improve the quality of the micrographs. Then, the local ACED which can adaptively utilize the local threshold values is implemented for image edge detection. After that, the modified CHT is presented to accurately recognize the circular particles. Figs. 2, 3, 5 and 6 demonstrate an example of the outputs of each step where the above image processing algorithm is implemented. A detailed description of the proposed algorithm is introduced as follows.

2.1. Preprocessing

The image preprocessing involves graying and denoising. Since only
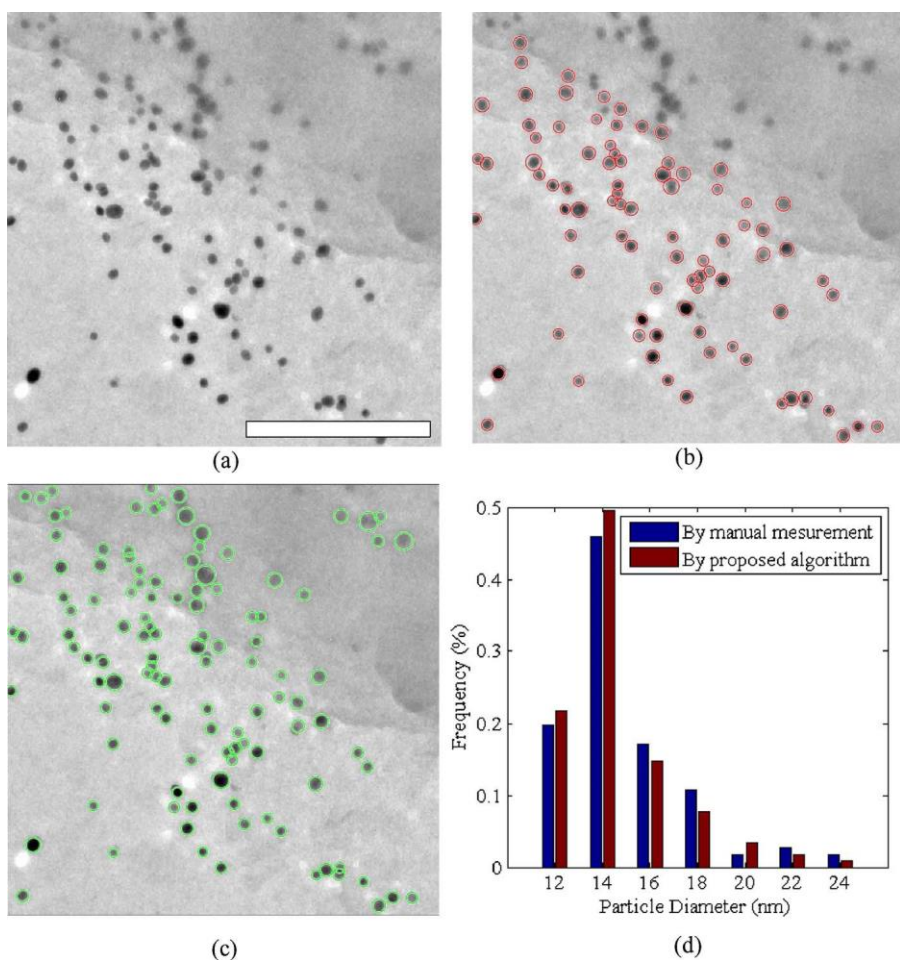
Fig. 7. (a) Original image of palladium nanoparticles deposited on pristine graphene (Vats et al., 2016). (b) Overlapped image of the original image and the result by applying global ACED. (c) Overlapped image of the original image and the result by applying our algorithm. The image is segmented into 7×7 sub-images. (d) Comparison of the particle size distributions by manual measurement and by our algorithm. Scale bar = 250 nm.

morphologic information is needed during particle detection, gray processing is applied here to eliminate color information so as to reduce the complexity of operation.

Denoising is a very important step to reduce statistical perturbations and recover some underlying signals. Typically, an image may involve four types of noise, namely salt and pepper noise, Gaussian noise, speckle noise and Poisson noise. There have been several filters to denoise image, including linear space filter, non-linear space filter, frequency filter and so on, among which median filter, a kind of non-linear space filter, has been widely used to remove salt and pepper noise due to its effective noise suppression ability and high computational efficiency (Yazdi and Homayouni, 2010). The main process of median filter is to run through the image pixel by pixel and replace each pixel with the median of filter window. In addition, median filter can also attenuate speckle noise and Poisson noise to some extent (Goyal et al., 2002). For the microscopy images, salt and pepper noise has been generally observed (Shanmugavadivu and Jeevaraj, 2014). Thus, median filter has been adopted in our algorithm to filter out the image noise. In local ACED, Gaussian filter will be adopted to suppress Gaussian noise, which will be applied in the next part.

Fig. 2a presents the original SEM image of porous hollow carbon nanospheres synthesized by He et al. (2013). The image shows a large number of overlapped particles and uneven background, which is even very difficult to separate and measure by eyes. Fig. 2b is the output after graying and median filtering. As is shown in the image, median filter can effectively preserve the important image characteristics, and at the same time, remove the pixels which stand out from their surrounding pixels. However, it also needs to be mentioned that it can result in a slight decrease in the image sharpness.

2.2. Local adaptive Canny edge detection

Image edge is an important feature for computer vision algorithms. Several edge detection operators have been developed, such as Roberts, Prewitt, Kirsch, Sobel, Robinson, Canny and so on (Muthukrishnan and Radha, 2012). Compared with the other edge detection algorithms, Canny edge detection can provide much better and more reliable edge detection results, and it has become the criterion for evaluating other methods.

Canny edge detection is based on a multistage algorithm, and two key thresholds, high threshold T_h and low threshold T_l, are adopted to detect and connect edges (Canny, 1986). Traditionally, the two threshold values require human intervention, the proper values of which are usually difficult to choose for different images. Thus, ACED algorithms, whose T_h and T_l can be obtained automatically, have been developed. Lu et al. (2006) has proposed an improved method to set the thresholds according to the gray-scale histogram, but this method may cause some fake edges. Fang et al. (2009) applied Otsu algorithm to get T_h, and T_l is obtained by multiplying T_h by a coefficient less than one, specifically 0.5. This method has been proved as an effective way for edge extraction. However, it has to be noticed that the adopted two threshold values mentioned above are two global values, which are obtained based on the whole image. For images with uneven background, this method may lose some local characteristics. To improve the accuracy of ACED, a local ACED, which can utilize the local T_h and T_l, has been developed to detect the object edges.

Detailed steps of the proposed local ACED are as follows:

1. Select how many sub-images to use and automatically segment the whole image into the required number.
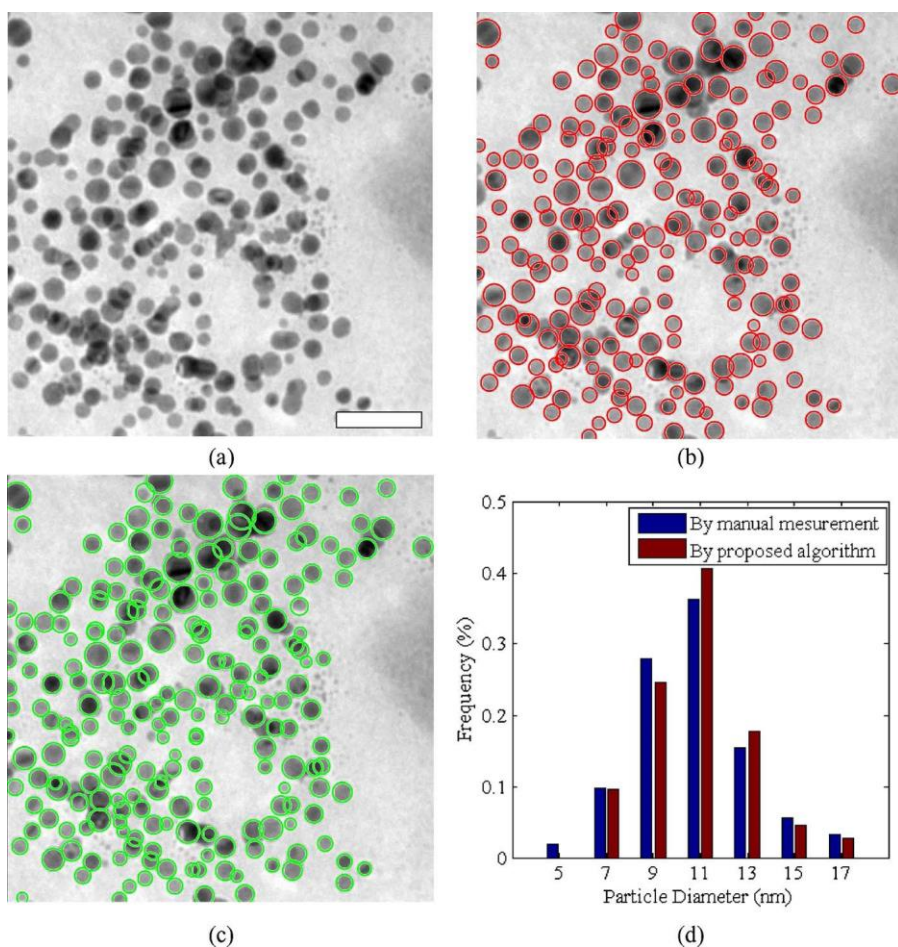
Fig. 8. (a) Original image of silver nanoparticles (Jiao et al., 2014). (b) Overlapped image of the original image and the result by applying global ACED. (c) Overlapped image of the original image and the result by applying our algorithm. The image is segmented into 8×8 sub-images. (d) Comparison of the particle size distributions by manual measurement and by our algorithm. Scale bar = 50 nm.

2. Calculate local T_h and T_l of each sub-image, individually. T_h is obtained by Otsu algorithm, while based on our experiments, T_l is settled as $0.4T_h$. Same coefficient has been adopted by Lu et al. (2006) and Hou and Liu (2012).
3. Apply Gaussian filter to filter out Gaussian noise.
4. Calculate magnitude and direction of gradient.
5. Apply non-maximum suppression to gradient value. This step will remove some non-edge pixels and extract candidate edges, the function of which is kind of like thinning edges because this step can highlight the most likely edge pixels and weaken other pixels.
6. Apply local T_h and T_l to detect and connect edges of each sub-image. A binary result can be produced after this step. If a pixel's gradient is higher than T_h, consider this pixel as an edge pixel. If a pixel's gradient is lower than T_l, mark this pixel as background. Otherwise, only mark this pixel as edge when it is connected to a pixel whose gradient is higher than T_h.
7. Merge the processed sub-images into an integrated image.

The edge detection results by adopting global ACED and local ACED are shown in Fig. 3. Fig. 3a presents the image without any segmentation and global T_h and T_l will be used. Fig. 3b illustrates the image by adopting local ACED. The image is segmented into 8×8 square subdivisions, and different T_h and T_l will be calculated within each subdivision individually. As is shown in the right column, compared with global ACED, although local ACED can cause discontinuity for some edges due to image segmentation, more edges can be detected, which can produced a more detailed binary result for the following processing.

2.3. Modified circular Hough transform

After the implementation of the local ACED, a binary result with detailed edge information will be generated. Then, a modified CHT will be adopted to detect circular particles from the binary result. Hough transform was initially proposed by Hough (1962) to detect geometric features, and the widely adopted Hough transform was invented by Duda and Hart (1972). The Hough transform is realized by a voting procedure in a special parameter space. The classic Hough transform is mainly designed for line detection, but later it has been expanded to identify other shapes (Ballard, 1981). CHT, a specialization of Hough Transform, has been proved as a powerful and effective way to detect circular objects.

The main principle of CHT is to transform geometric coordinates (x, y) into Hough parameter space. Hough parameter space contains three parameters, namely a, b and r, which can be obtained by the following equations.

$$(x - a)^2 + (y - b)^2 = r^2 \tag{1}$$

$$a = x - r \cdot \cos\theta \tag{2}$$

$$b = y - r \cdot \sin\theta \tag{3}$$

where θ is the angle upwards from the x axis, (a, b) is the circle center and r is the circle radius. Each point of a circle in geometric coordinates will vote for one point in Hough parameter space. An accumulative matrix based on votes in Hough parameter space will be constructed. Points which have high number of votes in Hough parameter space will be corresponded to circle candidates in geometric coordinates.

However, the above standard CHT requires a three dimensional space (a, b, r) to process images, which results in a low computation
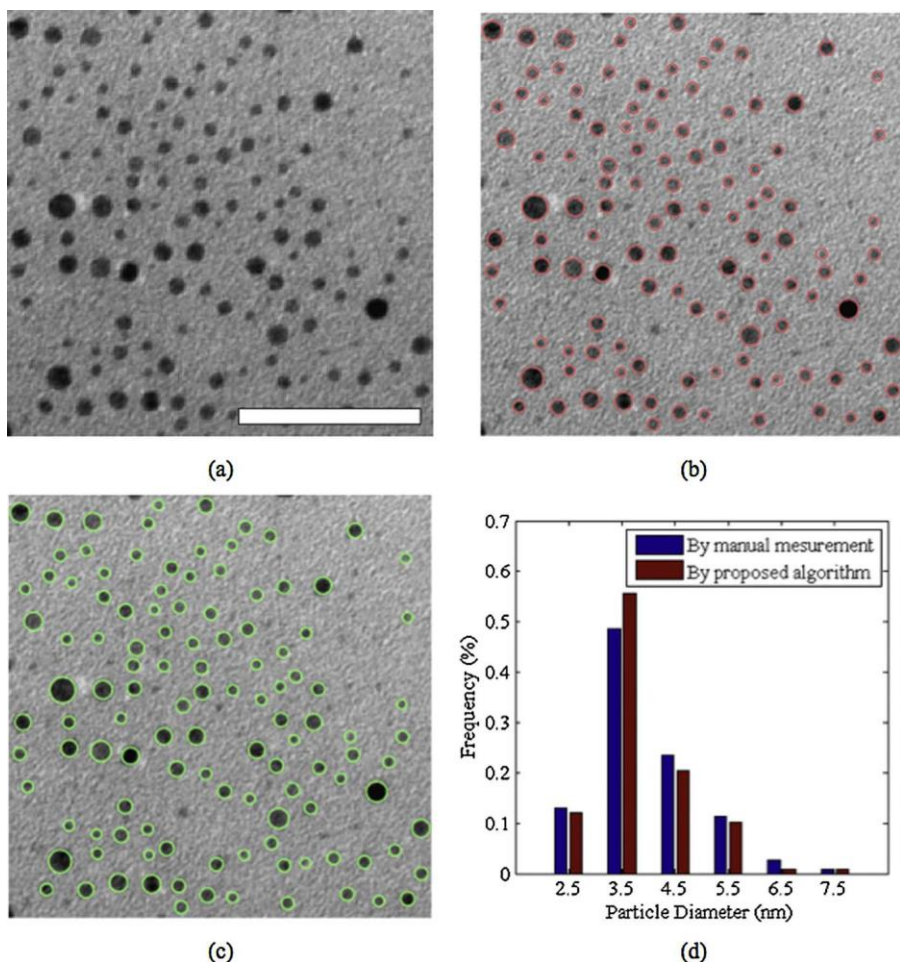
Fig. 9. (a) Original image of the well-dispersed silver nano-particles reduced by sodium borohydride in the presence of gelatin (Sivera et al., 2014). (b) Overlapped image of the original image and the result by applying global ACED. (c) Overlapped image of the original image and the result by applying our algorithm. The image is segmented into 7×7 sub-images. (d) Comparison of the particle size distributions by manual measurement and by our algorithm. Scale bar = 50 nm.

speed and a large storage space. To improve its performance, a modified CHT, two-stage Hough transform, which can speed up the computation, has been proposed by Yuen et al. (1990). The modified CHT mainly decomposes the standard CHT into two stages, a two dimensional accumulative matrix to find the circle center (a, b) and a one dimensional histogram to determine circle radius r. Fig. 4a and b demonstrate the two stages of the modified CHT, respectively. In Hough parameter space, the first stage will integrate all values along the radius axis at a single value of (a, b). An accumulative matrix will be generated, the local peaks of which will be regard as the circle centers. In the second stage, constrained by circle center (a, b) and Eq. (1), a radius histogram will be obtained for each candidate circle center, the peak of which is the desired radius. In spite of adding an additional step, this method can save the overall computation speed and storage space, especially for dealing with particles with a large radius range.

The realization of modified CHT is presented as follows:

1. Calculate accumulator matrix. Every pixel (x, y) will be calculated to vote for parameter (a, b).
2. Determine the centers of circles. The local peak values of the accumulator matrix will be regarded as the circle centers.
3. Determine the radius by radius histogram around each circle center.

Fig. 5a and b shows the overlapped images of the circle detection result and original image by implementing modified CHT to the binary results of Fig. 3a and b, respectively. Same sensitivity value of detecting circles has been applied to ensure the fair and valid comparisons. It can be found that Fig. 5b which processes the binary image with more detected edges presents more detected circles. Overall, the detected

circles for Fig. 5a and b is 123 and 141, separately.

2.4. Postprocessing

After the above process, parameters (a, b, r) of each particle will be stored. The particles' mean radius and size distribution can be obtained. The automatic detection results will be further compared with the data acquired by manual measurement.

Fig. 6 presents the particle size distributions by manual measurement and by our algorithm which adopts local ACED. The figure shows that the particle size distributions of the two measurements are in high agreement with each other. The number of particles detected by manual measurement is 133, which is less than the number recognized by our proposed algorithm. This is because the particles are highly overlapped in the image, which induces some circles hard to be distinguished by manual measurement. In addition, for some particles that are overly truncated at the border of the image or mostly occluded by others, they are not included in manual measurement. The mean diameters for manual measurement and the proposed algorithm are quite close, 178.20 nm and 176.58 nm, respectively.

3. Results and discussion

To further verify our algorithm, three other examples with different degrees of overlapped particles and uneven backgrounds are analyzed. The results generated by applying local ACED have been compared with the results produced by applying global ACED. To ensure valid comparison, when applying the modified CHT, same sensitivity value has been adopted.

Fig. 7a is the original TEM image of palladium nanoparticles deposited on pristine graphene (Vats et al., 2016). The image shows a very complex background with many veins of graphene and some particles do not stand out. Fig. 7b and c are the processed images by applying global ACED and by applying our algorithm, respectively. It can be found that when applying global ACED to the image, nearly 25% particles are missed, the detection result of which is unacceptable. By contrast, our algorithm which applies local ACED demonstrates a much better recognition and only few particles are not detected. The particle size distributions by manual measurement and by our algorithm are illustrated in Fig. 7d. The number of particles detected by the proposed algorithm is 115 with a mean diameter of 14.54 nm, while the same parameters by manual measurement are 111 and 14.92 nm respectively. Besides some undetectable particles for counting by eyes, the other reason behind this difference is that some particles are not in perfect circular shape and CHT may split them into two circles to match the most region of these particles.

The next example presented in Fig. 8a is the TEM image of silver nanoparticles (Jiao et al., 2014). The nanoparticles in this image show un-uniform contrast from the background and this image is very blurred and includes some overlapped particles. Fig. 8b and c are the circle detection results. Compared with Fig. 8b, c which utilizes the global threshold values can identify 206 particles, which is less than our proposed algorithm. The size distributions of the nanoparticles are given in Fig. 8d. Our proposed method can recognize 219 particles with a mean diameter of 10.84 nm. According to the manual measurement, these values are 215 and 10.74 nm. Only a small error between the two measurements can be observed.

Fig. 9a shows the TEM image of the well-dispersed silver nanoparticles reduced by sodium borohydride in the presence of gelatin (Sivera et al., 2014). The image is very grainy, some particles in which are even very hard to be recognized by manual measurement. Considering the background is relatively even, the detected numbers presented in Fig. 9b and c are both 117. Fig. 9d illustrates the size distributions which are obtained by manual measurement and by our proposed algorithm. The detected particle number by manual count is 115 which is two less than the automatic measurement's, while the mean diameters are 4.02 nm and 3.84 nm respectively. This error can be attributed to the indiscernible particle edges shown in the image.

4. Conclusions

To manually obtain the particle size distribution from SEM or TEM images is inefficient and can bring some potential subjective errors. To address this problem, an image processing algorithm which can automatically measure the particle size in different noises, overlapped particles and uneven backgrounds has been developed in this paper. Apart from some pre and post processing procedures, the main process of the proposed algorithm is based on local ACED and modified CHT. The local ACED can utilize the local threshold values, specifically T_h and T_l, within each sub-image to get the detailed binary edge detection results. Afterwards, the modified CHT which simplifies the computation complexity is adopted to speed up the recognition of circular particles. Results generated by the proposed algorithm are in good agreement with the manual measurements. Only small errors are observed in regards of the detected number and mean diameter. The robust and efficient algorithm can measure the particles with high precision, and it can be applied in the statistical analysis of large numbers of micrographs, especially for the micrographs with complex backgrounds.

Conflict of interest

The authors have no competing interests to declare. "None".

References

Ballard, D.H., 1981. Generalizing the hough transform to detect arbitrary shapes. Pattern Recogn. 13, 111–122.

Baudouin, D., Rodemerck, U., Krumeich, F., de Mallmann, A., Szeto, K.C., Ménard, H., Veyre, L., Candy, J.-P., Webb, P.B., Thieuleux, C., Copéret, C., 2013. Particle size effect in the low temperature reforming of methane by carbon dioxide on silica-supported Ni nanoparticles. J. Catal. 297, 27–34.

Blanco, E., Shen, H., Ferrari, M., 2015. Principles of nanoparticle design for overcoming biological barriers to drug delivery. Nat. Biotechnol. 33, 941–951.

Canny, J., 1986. A computational approach to edge detection. IEEE Trans. Pattern Anal. Mach. Intell. 8, 679–698.

Cervera, G.L., Ozkaya, D., Duninborkowski, R.E., 2011. A simple algorithm for measuring particle size distributions on an uneven background from tem images. Ultramicroscopy 111, 101–106.

Chinen, A.B., Guan, C.M., Ferrer, J.R., Barnaby, S.N., Merkel, T.J., Mirkin, C.A., 2015. Nanoparticle probes for the detection of cancer biomarkers, cells, and tissues by fluorescence. Chem. Rev. 115, 10530–10574.

Couvreur, P., 2013. Nanoparticles in drug delivery: past, present and future. Adv. Drug Deliv. Rev. 65, 21–23.

Dastanpour, R., Rogak, S.N., 2014. Observations of a correlation between primary particle and aggregate size for soot particles. Aerosol Sci. Technol. 48, 1043–1049.

Dastanpour, R., Boone, J.M., Rogak, S.N., 2016. Automated primary particle sizing of nanoparticle aggregates by tem image analysis. Powder Technol. 295, 218–224.

De Temmerman, P.-J., Verleysen, E., Lammertyn, J., Mast, J., 2014. Semi-automaticsize measurement of primaryparticles in aggregated nanomaterials bytransmission electron microscopy. Powder Technol. 261, 191–200.

Duda, R.O., Hart, P.E., 1972. Use of the Hough transformation to detect lines and curves in pictures. Commun. ACM 15, 11–15.

Fang, M., Yue, G., Yu, Q., 2009. The study on an application of otsu method in canny operator. Int. Symp. Inf. Process. 109–112.

Goyal, G., Singhal, M., Bansal, A.K., 2002. Comparison of denoising filters on colour tem image for different noise. Int. J. Image Process. Vision Sci. 1.

He, G., Evers, S., Liang, X., Cuisinier, M., Garsuch, A., Nazar, L.F., 2013. Tailoring porosity in carbon nanospheres for lithium-sulfur battery cathodes. Acs Nano 7, 10920–10930.

Hemachander, S., Verma, A., Arora, S., Panigrahi, P.K., 2006. Locally adaptive block thresholding method with continuity constraint. Pattern Recognit. Lett. 28, 119–124.

Hou, X., Liu, H., 2012. Welding image edge detection and identification research based on canny operator. International Conference on Computer Science and Service System, IEEE 250–253.

Hough, P.V., 1962. Method and Means for Recognizing Complex Patterns. (US3069654).

Houshiar, M., Zebhi, F., Razi, Z.J., Alidoust, A., Askari, Z., 2014. Synthesis of cobalt ferrite (CoFe2O4) nanoparticles using combustion, coprecipitation, and precipitation methods: a comparison study of size, structural, and magnetic properties. J. Magn. Magn. Mater. 371, 43–48.

Jiao, Z.H., Li, M., Feng, Y.X., Shi, J.C., Zhang, J., Shao, B., 2014. Hormesis effects of silver nanoparticles at non-cytotoxic doses to human hepatoma cells. PLoS One 9, e102564.

Jones, L., Nellist, P.D., 2013. Identifying and correcting scan noise and drift in the scanning transmission electron microscope. Microsc. Microanal. 19, 1050–1060.

Lappalainen, T., Lehmonen, J., 2012. Determinations of bubble size distribution of foam-fibre mixture using circular hough transform. Nordic Pulp Paper Res. J. 27, 930–939.

Lovell, E.C., Scott, J., Amal, R., 2015. Ni-SiO2 catalysts for the carbon dioxide reforming of methane: varying support properties by flame spray pyrolysis. Molecules 20, 4594–4609.

Lu, J.W., Ren, J.C., Lu, Y., Yuan, X.H., Wang, C.G., 2006. A modified canny algorithm for detecting sky-sea line in infrared images. Intelligent Systems Design and Applications (ISDA). 2006 Sixth International Conference on (Vol. 2). IEEE 289–294.

Mirzaei, M., Rafsanjani, H.K., 2017. An automatic algorithm for determination of the nanoparticles from TEM images using circular hough transform. Micron 96, 86–95.

Mohammadi, A., Barikani, M., Barmar, M., 2013. Effect of surface modification of Fe3O4 nanoparticles on thermal and mechanical properties of magnetic polyurethane elastomer nanocomposites. J. Mater. Sci. 48, 7493–7502.

Muller, D.A., Kirkland, E.J., Thomas, M.G., Grazul, J.L., Fitting, L., Weyland, M., 2006. Room design for high-performance electron microscopy. Ultramicroscopy 106, 1033–1040.

Muthukrishnan, R., Radha, M., 2012. Edge detection techniques for image segmentation. Int. J. Comput. Sci. Inf. Technol. 3, 250–254.

Pandey, J.K., Nakagaito, A.N., Takagi, H., 2013. Fabrication and applications of cellulose nanoparticle-based polymer composites. Polym. Eng. Sci. 53, 1–8.

Pei, S.C., Horng, J.H., 1995. Circular arc detection based on hough transform. Pattern Recognit. Lett. 16, 615–625.

Reske, R., Mistry, H., Behafarid, F., Roldan, C.B., Strasser, P., 2014. Particle size effects in the catalytic electroreduction of CO2 on Cu nanoparticles. J. Am. Chem. Soc. 136, 6978–6986.

Rizon, M., Yazid, H., Saad, P., Yeon, A., Saad, A.R., 2005. Object detection using circular hough transform. Am. J. Appl. Sci. 2, 1606–1609.

Shanmugavadivu, P., Jeevaraj, P.E., 2014. A robust fuzzy-based modified medianfilter for fixed-value impulse noise. In: The 8th International Conference OnRobotic, Vision,

Signal Processing and Power Applications. Springer. pp. 229–236.

Shi, J., Chan, C., Pang, Y., Ye, W., Tian, F., Lyu, J., Zhang, Y., Yang, M., 2015. A fluorescence resonance energy transfer (FRET) biosensor based on graphene quantum dots (GQDs) and gold nanoparticles (AuNPs) for the detection of mecA gene sequence of Staphylococcus aureus. Biosens. Bioelectron. 67, 595–600.

Sivera, M., Kvitek, L., Soukupova, J., Panacek, A., Prucek, R., Vecerova, R., Zboril, R., 2014. Silver nanoparticles modified by gelatin with extraordinary pH stability and long-term antibacterial activity. PLoS One 9, e103675.

Smereka, M., Duleba, I., 2008. Circular object detection using a modified Hough transform. Int. J. Appl. Math. Comput. Sci. 18, 85–91.

Sun, Y., Cai, Z., 2014. An improved character segmentation algorithm based on local adaptive thresholding technique for chinese nvshu documents. J. Networks 9, 1496–1501.

Tanhaei, B., Ayati, A., Lahtinen, M., Sillanpää, M., 2015. Preparation and characterization of a novel chitosan/Al2O3/magnetite nanoparticles composite adsorbent for kinetic, thermodynamic and isotherm studies of methyl orange adsorption. Chem. Eng. J.

259, 1–10.

Trandafilović, L.V., Božanić, D.K., Dimitrijević-Branković, S., Luyt, A.S., Djoković, V., 2012. Fabrication and antibacterial properties of ZnO-alginate nanocomposites. Carbohydr. Polym. 88, 263–269.

Vats, T., Dutt, S., Kumar, R., Siril, P.F., 2016. Facile synthesis of pristine graphene-palladium nanocomposites with extraordinary catalytic activities using swollen liquid crystals. Sci. Rep. 6, 33053.

Woehrle, G.H., Hutchison, J.E., Özkar, S., Finke, R.G., 2006. Analysis of nanoparticle transmission electron microscopy data using a public-domain image-processing program, image. Turk. J. Chem. 30, 1–13.

Wu, L.C., Yu, C., 2012. Powder particle size measurement with digital image processing using matlab. Adv. Mater. Res. 443–444, 589–593.

Yazdi, H.S., Homayouni, F., 2010. Impulsive noise suppression of images using adaptive median filter. Int. J. Signal Processing, Image Process. Pattern Recogn. 3.

Yuen, H.K., Princen, J., Illingworth, J., Kittler, J., 1990. Comparative study of Hough transform methods for circle finding. Image Vision Comput. 8, 71–77.